DOI: 10.61782/fa.2023.0617

BENDING OF SOUND WAVES IN THE VICINITY OF POROUS MATERIALS

A. Yürek, J. Heldmann, and T. Lokki
Acoustics Lab, Department of Information and Communications Engineering, Aalto University, Otakaari 5A, 02150 Espoo, Finland

ABSTRACT

The change in speed of sound in adjacent media redirects the sound waves. It is well known that when the temperature of the air changes gradually, the sound waves bend towards colder air with a lower speed of sound. However, not much is known about how sound waves bend close to a sudden change in speed of sound, e.g., in the vicinity of absorptive materials. Previous research, done in 1937, proposed that sound waves at 200 Hz bend prior to and upon penetrating a porous material. This paper replicates the old measurement with multiple tones at wide frequency range and presents an investigation procedure for the bending of sound waves propagating inside and in the close vicinity of acoustic absorbers. A set of measurements was carried out in the anechoic chamber using 16 MEMS microphones in two layers, forming eight pairs and positioned at different heights above and inside the horizontally placed absorbing material. At varying elevations, a three-way point source emitted tones in grazing angle in one-third octave bands. As in the original article, the evidence of bending sound waves is shown by delaying the top layer of microphones and estimating the time delay that minimizes the sum signal of microphone pairs when the phase of the top microphones is inverted. The results indicate that the apparent bending of sound waves varies with the adjacent absorbing material and is frequency dependent. In contrast to previous results, the bending seems to be almost unaffected by the grazing angle.

**Corresponding author*: *arif.yurek@aalto.fi.*

Keywords: *bending sound waves, refraction, porous materials, absorber, bio-materials.*

1. INTRODUCTION

Porous sound-absorbing materials have widespread use in many settings where an acoustic treatment is inevitable. Unlike resonant absorbers such as Helmholtz resonators or membrane absorbers, which can be tuned to specific narrow-bands, porous absorbers work over a wider bandwidth of frequencies. Absorption refers to the phenomenon of energy dissipation occuring when the incident sound energy is converted into heat by a series of viscous and thermal phenomena within the material [1]. The sound absorption coefficient, α, characterises a material's capacity for acoustic absorption and is an apparent indicator of the present setting, including the acoustic state, the geometry and mounting of the material sample [2].

There are two standard procedures for the measurement of the absorption coefficient. The impedance tube method is limited to normal sound incidence and materials for which a small sample can be regarded as indicative of the entire lining, whereas the reverberation chamber technique is used for random sound incidence and performed in diffuse field that is typical for many practical applications [3]. Alternatively, the angle-dependent absorption of sound in porous absorbers was investigated by Cucharero et al., and the results revealed that when the angle of incidence approaches normal incidence, the absorption curves draw close to the impedance tube results, while the grazing angle results approach diffuse field figures [4]. The findings exhibit that the measurements of angle-dependent absorption fit quite well between the results of two standard methods and that the absorption response of porous materials changes based on the angle of incidence. There-

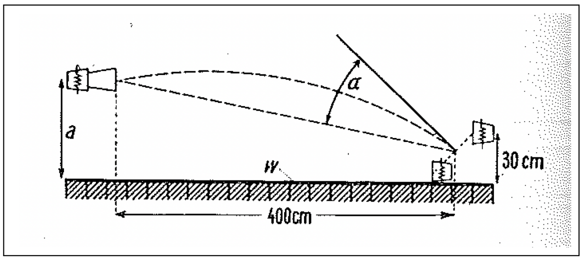

Figure 1. The original experimental setup in 1937.

fore, comprehending both the sound field and the propagation of acoustic waves in the close vicinity of materials is of great importance in the characterization of acoustic absorbers and their performance.

Changes in the propagation medium or variations in atmospheric parameters like air temperature or wind velocity can result in the refraction of sound waves, which is a common physical phenomenon [5]. The index of refraction, which is a material property, can take on either a positive or negative value when travelling among mediums, depending on whether the wave maintains its direction relative to the boundary [6]. Within the air, invisible boundaries formed by temperature gradients can cause sound waves to bend since the velocity of sound in air varies with temperature. In liquids, sound waves tend to refract while travelling up or down across the horizontal strata, for instance, in seawater with varying characteristics such as temperature, salinity, and pressure [7]. Refraction under water sometimes causes the sound to be trapped between two boundaries and travel large distances.

In a 1937 study, Janovsky and Spandöck argued that there is a 'false' air absorption close to the porous surfaces that is actually induced by the sound wave bending in the air on top of the absorptive material [8] (also briefly explained in [9] and [10]). By monitoring 200 Hz tones with changing angles of incidence, they found that a wave bending occurs towards the absorber. To achieve this, they placed a sound source at an adjustable height over the absorbing material (see Fig. 1). Then, one microphone was placed 4 metres away from the source and immediately on top of the absorbing material, while a second, horizontally adjustable microphone was positioned 30 cm above the floor on top of the other. When the source emitted tones at 200 Hz, the input of one of the microphones was inverted, and the signals were added up. Finally, by moving the top one, they attempted to determine the horizontal distance needed between the two microphones for maximal signal attenuation. The attenuation was verified by connecting the sum signal to 20 telephone lines, asking 20 subjects to listen to the telephones, and estimating when the attenuation was maximal. The results for several loudspeaker heights revealed that the angle α decreases with increasing source height.

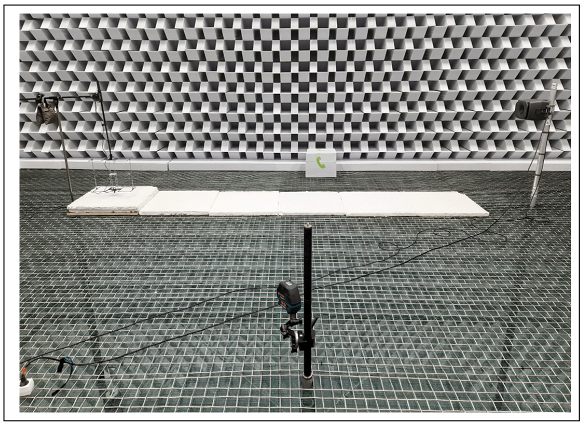

Figure 2. General measurement setup with six bioboard panels lined on the walking net.

The current study replicates the nearly century-old experiment to investigate the variables that influence the bending of sound waves in the vicinity of porous absorbers. To do this, we used a wider range of tones, an array of 16 microphones, and a variety of different porous samples with varying thickness and quantity, including a novel bio-based absorber in addition to commercially available acoustic panels. To explore the bending of the sound waves, we used eight pairs of microphones that captured a sequence of tones emitted from a vertically adjustable loudspeaker. Then, we digitally computed the delay that minimises the sum of the signals for each pair. Our findings suggest that the angle of wave bending depends on the adjacent porous material and the frequency of the sound. Contrary to previous research, it appears that the bending does not depend on the elevation of the loudspeaker for close-to-grazing-angle sound waves.

2. MATERIALS AND METHODS

2.1 Experimental Setup

The measurements are carried out in the large anechoic chamber of the Aalto Acoustics Lab. The room has inner dimensions of $8200\,\mathrm{mm} \times 8200\,\mathrm{mm}$ (width x length), and its height is $7200\,\mathrm{mm}$ (from the floor wedge tip to

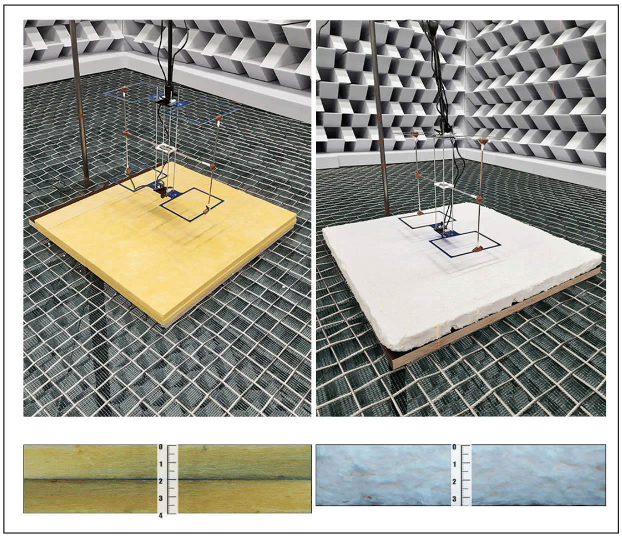

Figure 3. Glass-wool sample and thickness (on the left), bioboard sample and thickness (on the right).

the ceiling wedge tip). Thus, the chamber size allowed for the recreation of the original setting with a speaker-to-microphone distance of 4 metres, as can be seen in Fig. 2. The walking net is located 2940 cm above the floor wedge tips. The microphone array, the source, and the laser level were installed on the existing floor supports for mounting measurement equipment.

For the assessment of sound wave bending, two porous materials are used: glass-wool and bioboard (see Fig. 3). The latter is a novel bio-based sound absorber that is made from biofibres and is mostly composed of wood-based cellulosic fibres and bio-based binders [4]. Such environmentally friendly materials, which bind atmospheric CO_2 for decades when installed in buildings, would be a welcomed alternative to traditional absorption materials.

We used tiles of 3.5-cm bioboard and 2-cm glass-wool. Absorber samples placed under the microphone array were mounted horizontally on a rigid wooden plate (68× 68 cm) without any mechanical connection; however, no rigid plate is installed under the additional tiles. The absorption coefficients given in Fig. 4 are measured using a three-microphone impedance tube technique and in accordance with the standard ISO 10534-2. The absorption contours are obtained by averaging the results of three samples for each material.

By combining four modules, each having four MEMS microphones (UMIK-X Distributed Microphone Array),

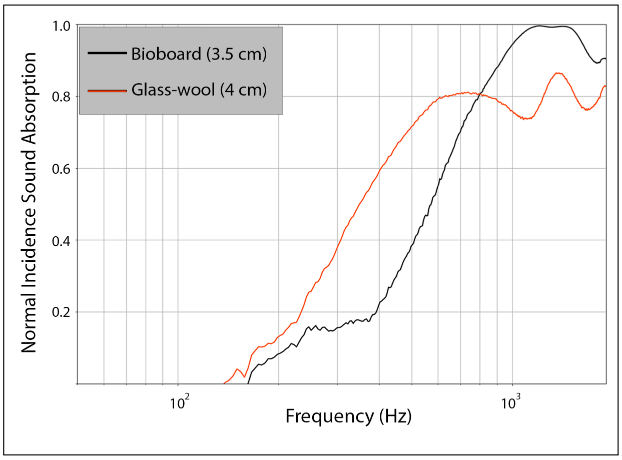

Figure 4. The absorption coefficients of the samples.

we obtained a setup of sixteen receivers arranged in two horizontal grids of eight. This enabled us to have eight pairs of receivers distributed horizontally. The upper and lower grids were 30 cm apart. With a single twisted-pair cable running the A2B protocol at 48 kHz, all the modules were daisy-chained. The array was suspended on top of the absorbing material from an adjustable mount that allowed for the capture of sound signals at various heights above the porous samples. With this setup, we could place the absorption materials underneath the microphone array and investigate the bending of sound waves by analysing the signals from the microphones.

Fig. 5 depicts the primary elevations and relative positions of the source, the receiver array, and the absorbent tiles. In the present setup, the receiver elevation refers to the height of the intermediate axis between the upper and lower microphone grids, whereas the source elevation denotes the level of the loudspeaker acoustic axis. Given the 30-cm distance between the upper and lower microphone grids, the bottom layer has captured the signals at 15 cm below the intermediary axis, whereas the upper layer received them at 15 cm above. All elevations are given relative to a reference zero level. Although the indicated levels are referred to as the main positions of the experimental components, alternative elevations are also used in some measurements.

During the measurements, to avoid displacement of the microphones, the array was counterbalanced using a sandbag that was fixed to the mounting. To play the audio signals, a three-way coaxial loudspeaker with a flat frequency response of 58 Hz – 20 kHz was mounted on a

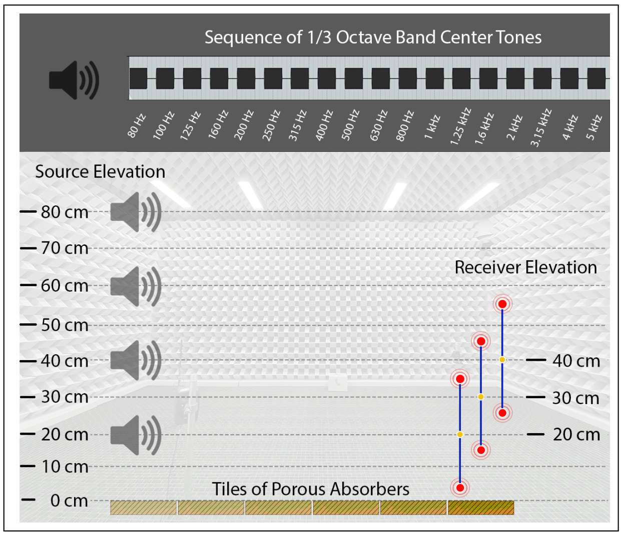

Figure 5. The sequence of one-third octave band center tones in time domain (at the top). Representation of main source, receiver and absorber positions (at the bottom).

cylindrical metallic bar four metres from the central vertical axis of the microphone grid. The internal gap of the bar was stuffed with foam-like materials to prevent any resonance. The aluminium clamp used to mount the loudspeaker allowed easy vertical movement along the bar by simply loosening one screw. Before each measurement, we used a laser level to check the levels and avoid any horizontal displacement of the array.

2.2 Computation of Sound Wave Bending

For each speaker-receiver position, an initial measurement without any absorptive or reflective object is carried out, i.e., the free field condition is measured. It was later used for the estimation of the angle of incidence and the possible initial time delay between paired microphone signals. The measurements with the bioboard and glass-wool tiles came after this. To investigate the influence of the absorbing surface area on sound wave bending, measurements are performed in multiple steps by altering the sample area while keeping the speaker and receiver positions stable. To achieve this, the number of absorbent tiles on the propagation path is increased by one (i.e., from one to six) at each step. In the final part of the measurements, by placing the lower grid in between two layers of bioboard, we assessed the bending within the porous medium.

For the computation of sound wave bending, we digitally analysed the time delay between paired microphones. A loudspeaker emitted a series of one-third octave band center tones ($80\,\mathrm{Hz}$ to $5\,\mathrm{kHz}$) about 4 metres away from the receivers. The tones were 2 seconds long and were separated by 1 second of silence. The signals are monitored in real time and recorded into separate channels in Reaper. After the rendering (24 bits, $48\,\mathrm{kHz}$ sampling rate), the audio files (WAV format) are transferred to MATLAB for digital signal processing.

In the present study, unlike the previous experiment, the upper and lower microphones remained stable along the horizontal axis. Instead, the upper layer signals are digitally delayed and subtracted from the bottom ones. After the subtraction, we computed the equivalent sound pressure level L_{eq} of the 1-second signal in the middle of each 2-second tone. The particular time delay ensuring the maximum cancellation for each pair is then determined. At each frequency, the final figures are acquired by averaging the four median values of eight microphone pairs.

3. RESULTS

3.1 Frequency Responses

In addition to recording the tones, the measurement sequence included a sweep for an impulse response measurement to study, e.g., the frequency responses of the microphones. The frequency responses illustrated in Fig. 6 are derived from the medians of upper and lower grid microphones in four specific configurations, including free field, bioboard with rigid plate, and glass-wool with and without rigid plate. In all cases, the microphone array remained in a fixed position at $20\,\mathrm{cm}$ (lower grid level: $5\,\mathrm{cm}$; upper grid level: $35\,\mathrm{cm}$); and the height of the loudspeaker varied between 20 and $80\,\mathrm{cm}$. The analysis is based on a comparison between the findings in free field and with materials. The results show that when an adjacent absorbing surface is present, the bottom grid microphones (close to the absorptive material) have a greater magnitude at $200-800\,\mathrm{Hz}$, whereas an energy loss is observed at frequencies over $800\,\mathrm{Hz}$. Furthermore, the attenuation over $1\,\mathrm{kHz}$ decreases as the angle of incidence rises due to the higher speaker position. Additionally, at low frequencies, the change in magnitude relative to free field conditions is limited to $\pm\,1\,\mathrm{dB}$, regardless of the incident angle.

The impact of the absorbent area on frequency attenu-

Figure 6. Frequency responses, median of all mics, four materials.

ation is investigated by altering the number of tiles on the propagation path. Fig. 7 shows the magnitude responses of upper and lower grid microphones when the number of bioboard panels is increased in steps from one to six. We explored this effect for two distinct source elevations, 25 cm and 85 cm. In both cases, the absorbent area does not have a clear impact on the frequency loss up to around 500 Hz. However, when the source height is close to that of the receiver, e.g., 25 cm, there is a significant loss of energy between 500 Hz and 1.5 kHz at all microphones. Subsequently, at mid-frequencies, attenuation is highly related to the absorbing area. Also, as the number of tiles increases, the attenuation on upper microphones is significant, and the peak shifts towards lower frequencies. The absorbent area, nevertheless, has no effect on the sound level drop when there is a 9 degree incidence (i.e., when the source elevation is 85 cm).

For the assessment of frequency attenuation and sound bending within the porous medium, we performed specific measurements by placing the bottom microphone grid inside a 7-cm bioboard. To accomplish this, we located the grid in between two layers of 3.5-cm bioboard and used a similar technique to analyse the microphone signals. The frequency responses of both microphone grids are computed for various angles of incidence (e.g., when the source elevation is 20 cm, 40 cm, 60 cm and 80 cm). As indicated by Fig. 8, which depicts the magnitude responses of lower-level microphones over the band of interest, there is a boost between 100 Hz and 500 Hz, while a gradual attenuation is observed beginning at 500 Hz.

3.2 Bending of Sound Waves

To investigate the sound wave bending over the porous samples, we estimated the equivalent sound pressure levels at each receiver, applied sample-based delay to the upper layer microphones, and then simulated the summation of out-of-phase signals by performing digital subtraction between paired receivers. For each pair and at each tone of interest, the 1-second L_{eq} of the sum signal is computed, and this procedure is repeated 20 times using sample-based time delays ranging from 1 to 20 samples. By this method, we determined the delay-length at which the L_{eq} is the minimum for each pair. Fig. 9 illustrates the delays and the corresponding angle of bending for two incidences (e.g., the source elevation is 20 cm and 80 cm, respectively). For comparison, we measured signals in the free field and when two different materials were placed under the receivers. The time delays presented in the graphs are estimated by sorting the levels of eight microphone pairs and then computing the mean of the median four pairs. In free field, the angle of incidence is near zero when the source and receiver have the same

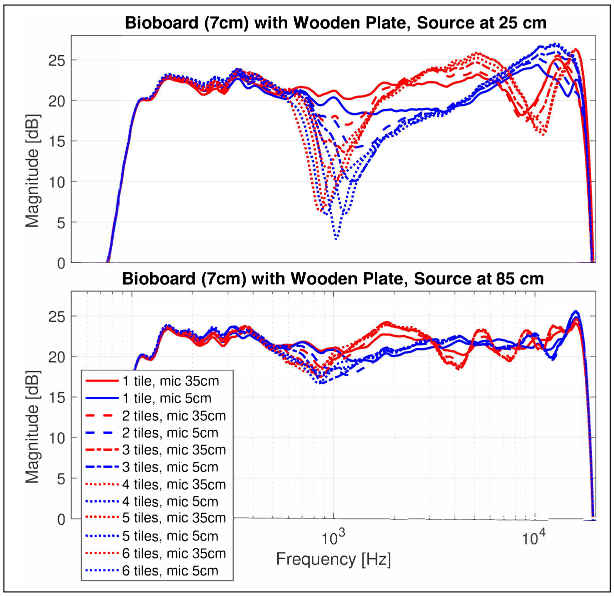

Figure 7. Frequency responses, median of all mics, the effect of tiles under the sound propagation path.

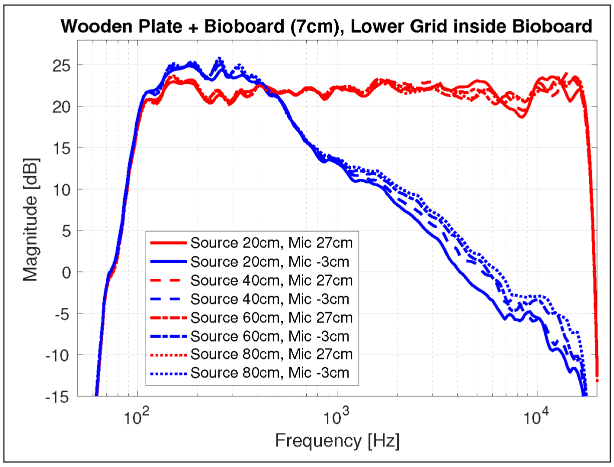

Figure 8. Frequency responses, median of all mics, lower level inside the material.

height, e.g., 20 cm. However, the angle of incidence increases up to 9 degrees when the source is located higher, e.g., at 80 cm. This is indeed according to the trigonometry of the measurement system [$\arctan(0.6/4.0) = 8.5^o$]. When the absorbent samples are in place, the bending towards the porous surface is prominent between 400 Hz and 1200 Hz in both scenarios. Intriguingly, a "negative"

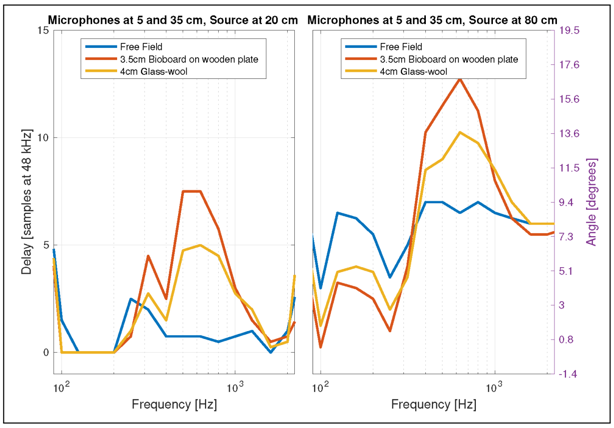

Figure 9. Example of results of how much top layer microphones must be delayed to minimize the sum.

bending appears from 200 Hz to 400 Hz, also in the case with no rigid plate under the sample. As the analysis is based on summed sinusoids, it appears that these low frequencies are partially reflected from the materials and then summed up in lower-level microphones, so that such "negative" bending is seen in the results.

Similar analyses are performed for a larger variety of incidence angles and changing receiver-to-absorber distances. This time, however, the results are free field compensated, meaning that the free field levels are subtracted from the measurements with materials; thus, the figures represent only the additional bending caused by the porous materials (see Fig. 10). In all cases, the angle of bending at low frequencies is negative, and there is hardly any bending above 1 kHz. The results reveal that the frequency range where the bending is prominent becomes narrower and shifts towards the low frequencies as the distance between the microphones and the absorption material increases.

The impact of the area of absorbent surface along the propagation path on sound wave bending is computed for one to six bioboard tiles and two distinct source elevations. Findings are depicted in Fig. 11. When the source and the microphones are located at the same height (i.e., 20 cm), and thus the sound waves propagate very close to the porous tiles, the bending occurs at frequencies from 125 Hz to 1.25 kHz, independent of the tile quantity. However, the more tiles, the stronger the bending between 500 Hz and 1000 Hz. When there are six tiles (i.e., the propagation path is almost completely lined), the bending angle reaches 22 degrees and is at its greatest. On the other

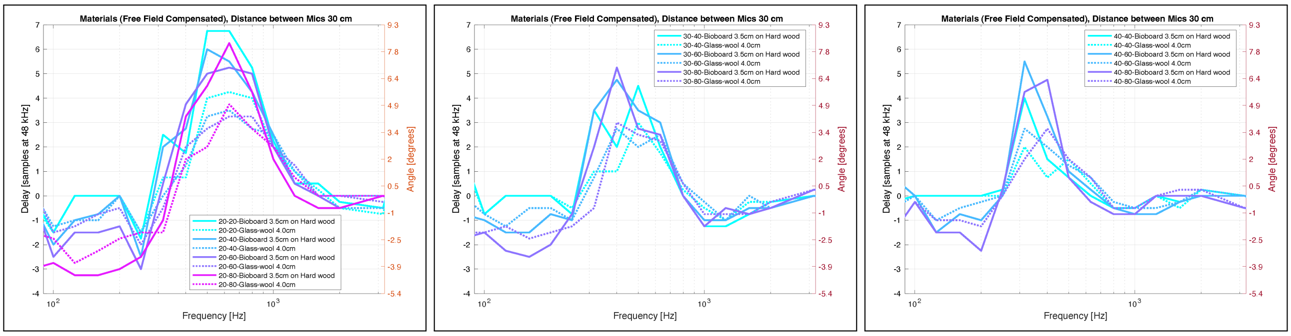

Figure 10. Results when free field conditions are compensated.

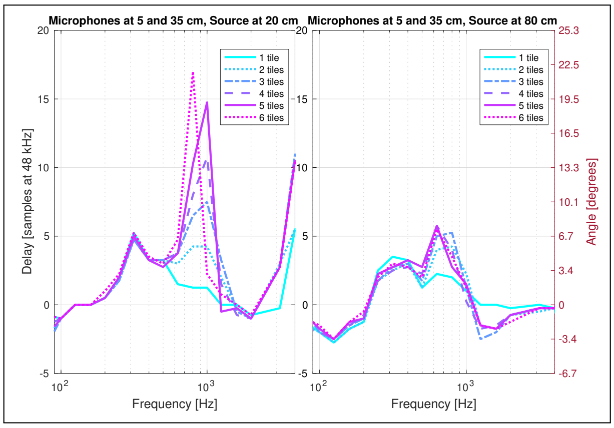

Figure 11. The effect of the extra bioboard absorption tiles under the sound transmission path.

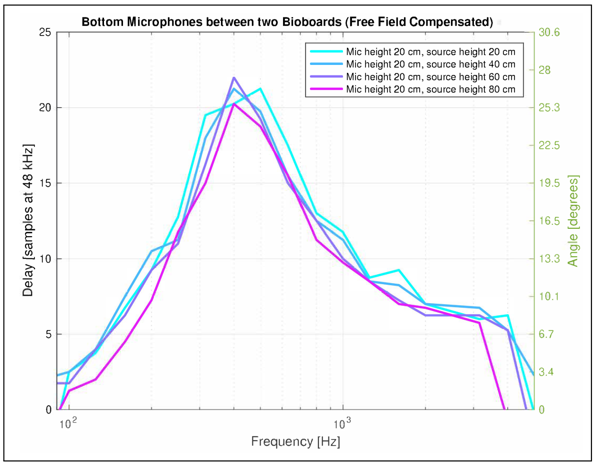

Figure 12. Sound wave bending when lower microphone grid is 3.5 cm inside the absorption material.

hand, when the source is positioned at 80 cm, the values are found to be very close to each other. Therefore, when the sound waves approach at a greater angle, the bending angle is almost unaffected by the absorbent area along the path.

When the source is located at 20 cm, the sound waves reach the absorbers at a very small angle, so possible reflections from the wooden plate do not encounter the receiver array. Contrarily, once the grazing angle is greater (i.e., the source is at 80 cm), some reflections from the rigid plate hit back at the bottom layer microphones, resulting in "negative" bending in our findings below 125 Hz and over 1 kHz.

Fig. 12 illustrates the free field compensated sound wave bending computed for varying incidences (i.e., the source is placed at 20 cm, 40 cm, 60 cm, and 80 cm) when the bottom microphone grid is placed in between two layers of 3.5-cm bioboard. The findings reveal that once the bottom-grid receivers are inside the absorbing medium, the bending is greater and a broader range of frequencies is influenced. The maximal bending occurs from 300 Hz to 500 Hz and is estimated to be between 25 and 28 degrees, regardless of the grazing angle.

4. DISCUSSIONS AND CONCLUSIONS

The original study [8] showed results only at 200 Hz, and the bending was substantial, ranging from 10 to 25 degrees depending on the source heights that we replicated here. In the present study, we did not find any bending at such low frequencies, but we did at higher frequencies. Our results also suggest that the bending is not really dependent on the incoming angle of the sound wave at grazing angles (0 to 9 degrees were studied here). Moreover, we found that the amount of bending is different for different materials. The reason for this is not fully understood and more research is needed.

Polack has derived a generalized formulation of sound propagation that takes into account the vicinity of absorption material [11]. This complex mathematical formulation has a free parameter for the thickness of the "adaptation layer" in which the bending of sound waves occurs. Polack proposes that this layer could be, e.g., a quarter wavelength, which is often hypothesized in room acoustics. In the presented results, bending still occurs when the lower microphones are 25 cm from the material, i.e., at 340 Hz (quarter wavelength), see Fig. 10. It should be noted that the frequency region of the bending waves gets narrower as the distance from the absorption material increases, and only the lower frequencies are bending farther away. The connection between the wave bending and absorption coefficient was not possible to find based on the obtained results, but it would be another interesting research topic in the future.

The presented results show that a frequency-dependent gradient of sound wave bending is apparent, which increases while the sound wave is approaching the porous material. In prior studies of sound propagation in different altitudes of air, changes in the speed of sound due to temperature and density gradients account for sound wave bending. However, none of those were present in this study, and the change in speed of sound between two media is abrupt. Also, viscous effects at the air-material boundary are too small to affect molecules at the measured distances where sound bending occurs. At 1000 Hz, the viscous-boundary layer for an acoustic wave impacting a rigid wall is merely 70 micrometres, while the bending has been measured at distances of dozens of centimeters.

Hence, possible causes for bending sound waves in the vicinity of porous absorbers are not yet fully understood. The measured impulse responses allowed us to estimate the speed of sound with cross-correlation between the first and last microphones. The analysis was performed for top and bottom layer microphones separately and by first filtering the measured IRs to 1/3 octave bands. The results, which are not presented here, demonstrate that when porous material is placed under the microphones, the speed of sound is frequency-dependent. The sound speed was lower in the bottom layer microphones at frequencies where sound wave bending was detected in this study by comparing tones. At other frequencies the speed was about 343 m/s in both the top and bottom layer microphones. Moreover, the changes in speed of sound were also apparent when the microphones were further away (15 cm and 25 cm) from the porous material and the frequency range was narrower, similar to the results depicted in Fig. 10. Future studies will involve denser measurement heights above the absorption material to determine the thickness of the layer of reduced speed of sound as a function of frequency.

Acknowledgements: This work was supported by the Academy of Finland Flagship project "FinnCERES" (318890 and 318891) and the KAUTE foundation.

5. REFERENCES

[1] M. A. Kuczmarski and J. C. Johnston, "Acoustic absorption in porous materials," 2011. NASA/Technical Memorandum 2011-216995.

[2] F. Fahy, *Foundations of Engineering Acoustics*. Elsevier Academic Press, 2001.

[3] M. Crocker, *Handbook of noise and Vibration Control*. John Wiley & Sons, 2007.

[4] J. Cucharero, T. Hänninen, and T. Lokki, "Angle-dependent absorption of sound on porous materials," *Acoustics*, vol. 2, pp. 753–765, 2020.

[5] T. Gabrielson, "Refraction of sound in the atmosphere," *Acoustic Today*, vol. 2, no. 2, pp. 7–17, 2006.

[6] B.-I. Popa and S. A. Cummer, "Negative refraction of sound," *Nature Materials*, vol. 14, no. 4, pp. 363–364, 2015.

[7] D. P. Nowacek, M. P. Johnson, and P. L. Tyack, "North atlantic right whales (eubalaena glacialis) ignore ships but respond to alerting stimuli," *Proceedings of the Royal Society of London Series B: Biological Sciences*, vol. 271, no. 1536, pp. 227–231, 2004.

[8] W. Janovsky and F. Spandöck, "Aufbau und untersuchungend eines schallgedämpften raumes," *Akustische Zeitschrift*, vol. 2, pp. 322–331, 1937.

[9] E. H. Bedell, "Some data on a room designed for free field measurements," *The Journal of the Acoustical Society of America*, vol. 8, pp. 118–125, 1936.

[10] L. Cremer and H. Müller, *Principles and Applications of Room Acoustics*, ch. I.6, Vol. 1, pp. 154–156. London, England: Applied Science Publishers, 1982.

[11] J.-D. Polack, "Generalized formulation for acoustics." Available at https://hal.science/hal-02148492/, 2019.